Chapter – 7

A correlation of crystalline perfection with SHG efficiency of urea doped ZTS single crystals

Abstract

The pure and doped single crystals of ZTS have been grown by slow evaporation solution technique. The incorporation of urea in the grown crystals has been confirmed and analyzed by Fourier transform infrared spectroscopy. The crystal structure of crystals has been confirmed by powder X-ray diffraction. The high resolution X-ray diffractometry revealed that the ZTS crystals could accommodate urea up to certain concentration without any deterioration in crystal lattice and above this concentration, very low angle structural grain boundaries were developed and the excess urea was segregated along the grain boundaries. At very high doping concentrations, the crystals were found to contain mosaic blocks. The relative SHG efficiency of the crystals was found to be increased substantially with the increase of urea concentration. The enhancement of second harmonic generation efficiency by urea doping in ZTS single crystals and its correlation with crystalline perfection has been investigated.

7.1 INTRODUCTION

In the era of fast communication and high density data, the design of devices that utilize photons instead of electrons in the transmission and storage of information has created a need for new materials with unique optical properties (Williams *et al.*, 1984). The nonlinear optical (NLO) materials have a significant impact on laser technology, optical communication, and optical data storage technology. The efforts have been made to produce novel frequency conversion materials primarily with increased magnitude of the NLO tensor (d_{ijk}) coefficients to produce structures that can cause frequency doubling with low peak power sources, such as diode lasers. The research is also focussed on the development of highly transparent crystals suitable for frequency conversion for high-power lasers, suitable for the inertial confinement fusion (Velsko *et al.*, (1988). In the race of invention of new NLO materials it is also equally important to enhance the NLO properties of the known materials by either the incorporation of functional groups (Sweta *et al.*, 2007; Ushasree *et al.*, 1999) or dopants (Bhagavannarayana *et al.*, 2008) of the available NLO materials, for tailor made applications.

Thiourea molecules are the analogs of urea with O replaced with S atom. It is nearly a coplanar in structure and possesses the resonant hybrid of three resonance structures shown in Fig. 7.1(a). It has the large dipole moment. The π-orbit electron delocalization in thiourea arises from the mesomeric effect and is responsible for the nonlinear optical response and absorption near the ultraviolet region. Thiourea is capable to make the complexes with ionic inorganic solids through the C=S bond. The series of metal-urea, thiourea (TU) and allylthiourea (ATU) have been explored such as; $Cd(TU)_2Cl_2$, $Cu(TU)_3Cl$, $Zn(TU)_2Cl_2$, $Cd(ATU)_2Cl_2$, $Cd(ATU)_2Br_2$, $Zn(ATU)_2Cl_2$ and known for many years which have been investigated for their NLO behaviors. These complexes exhibit the second harmonic generation (SHG) comparable to that of urea and are good in mechanical hardness and thermal stability as well.

Tris(thiourea)zinc sulphate ($Zn(TU)_3SO_4$; (ZTS)) is one of such coordination complexes of thiourea. A schematic for the molecular structure of ZTS is shown in Fig. 7.1(b). The crystal structure of ZTS for the first time was determined by

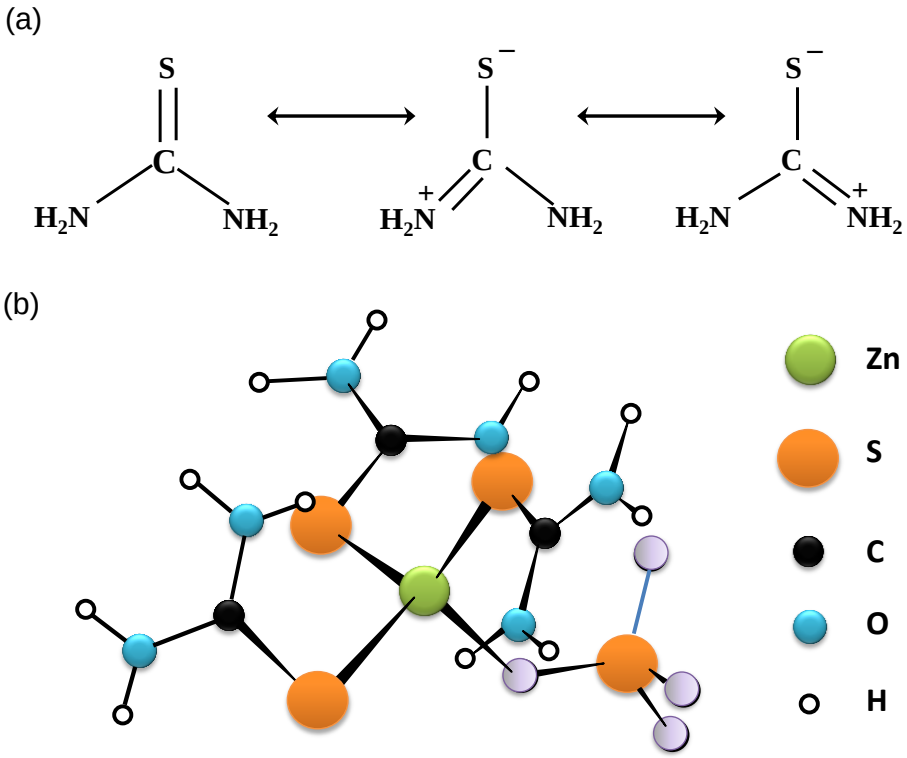

Fig. 7.1: *(a) The resonating structures of thiourea representing π-orbital electron delocalization, (b) the projection of a ZTS molecule shows the three thiourea sulphur atoms and a sulphate ion oxygen atom making the coordination bond with Zn^{2+} ion at the tetrahedral position*

single crystal X-ray determination method and it was reported by Andreetti *et al.*, (1968). It is a well characterized material of noncentrosymmetric orthorhombic crystal system with lattice parameters a = 11.126 Å, b = 7.773 Å and c = 15.491 Å and space group $Pca2_1$ (point group *mm2*). It exhibits a low angular sensitivity, and the SHG phenomenon for the first time was demonstrated by Marcy *et al.*, (1992). The SHG efficiency compared to that of potassium dihydrogen phosphate (Marcy *et al.*, 1992) was found to be ~2 times for 1064 nm fundamental wavelength. The extensive vibrational studies have been carried out on ZTS through Raman and Fourier transform infrared (FTIR) spectroscopy (Venkataramanan *et al.*, 1994). ZTS crystals are found to possess high laser damage threshold and wide optical transparency (Venkataramanan *et al.*, 1995). Thermal, elastic and electro-optic (Kerkoc *et al.*, 1996; Alex & Philip, 2001; Sastry, 1999) properties were also reported. The defects analysis of the pure ZTS crystals has been carried out by X-ray topography and its mechanical properties were also studied. The thermal properties of

ZTS single crystals have been studied and the thermal diffusivity of crystals measured using the laser flash method and the principal coefficient of thermal conductivity reported to be largest in the polar *c* crystallographic axis and smallest in *a*-axis. The thermal expansion coefficients measurements showed that the polar axis *c* contracted linearly as the temperature increased, whereas *a* and *b* expanded and inferred the presence of extensive intermolecular hydrogen bonding in ZTS between the $O(SO_4)$ and $N(NH_2)$ (Kerkoc *et al.*, 1996).

As it is clear from the structure of ZTS as shown in Fig. 7.1 there is a lot of space in the lattice of crystal and possibility of extensive hydrogen bonding. Different kinds of organic and metallic impurities have been used as dopants to improve the physical parameters of ZTS single crystals. In our recent studies, the transition metal (Mn^{2+}) doping lead to the enhancement in optical transparency as well as SHG efficiency and its influence on the crystalline perfection has been investigated (Bhagavannarayana, Kushwaha *et al.*, 2009). The organic dopants were used to modify the optical as well as the structural properties of ZTS crystals (Bhagavannarayana *et al.*, 2006; Sweta Moitra & Tanusree Kar, 2007). Better optical properties were found by mixing phosphate in ZTS crystals (Ushasree *et al.*, 1999). Our recent studies on ZTS (Bhagavannarayana *et al.*, 2008; Bhagavannarayana *et al.*, 2006) in the presence of some inorganic/organic dopants elucidated the enhancement of crystalline perfection which in turn leads to the improvement in the SHG efficiency.

In the present investigation, effect of urea (NLO material) doping in ZTS crystals has been studied, urea is one of the best SHG organic materials but due to its high hygroscopic nature it is not feasible to growth the bulk single crystals of it. Therefore, it has been planned to use urea as a dopant with different concentrations for the ZTS crystals, to enhance the SHG efficiency. The ZTS are easy to grow into bulk crystal form by solution method. Urea is having the amino groups and expected to make the extensive hydrogen bonding, which is also expected to increase the SHG behaviour. The grown single crystals were characterized by FTIR to confirm the functional groups and bonds and the presence of urea in doped ZTS crystals.

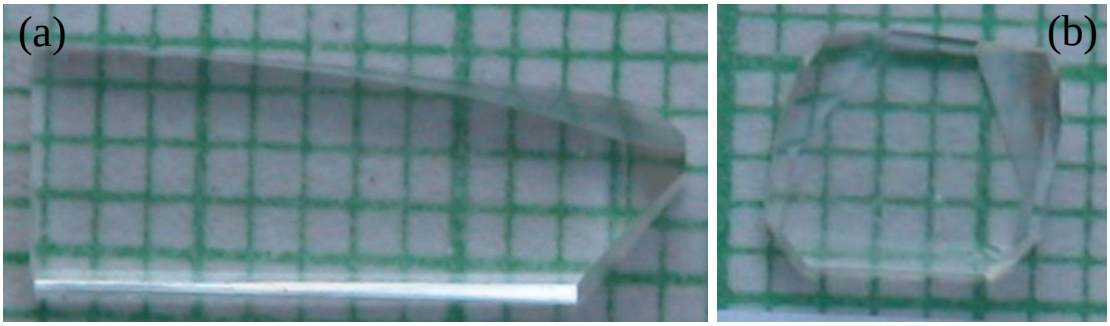

Fig. 7.2: *The photographs of (a) pure ZTS and (b) a typical urea (2.5 mol%) doped ZTS single crystals, grown by SEST*

The crystal structure of grown crystals was confirmed by powder X-ray diffractometry (PXRD). The crystalline perfection of undoped and urea doped crystals at different concentrations has been evaluated by high resolution X-ray diffractometry. The effect of urea doping on SHG efficiency was studied by Kurtz powder technique and the relative SHG values have been measured. An interesting correlation between the crystalline perfection and SHG efficiency is found and well discussed.

7.2 CRYSTAL GROWTH

The ZTS is a semiorganic material and decomposes on its melting therefore it is not feasible to grow the single crystals of ZTS by melt technique. However, it has good solubility in water therefore the slow evaporation solution technique (SEST) is a suitable technique for the growth of single crystals of it. The pure and doped crystals growth process has been demonstrated in *Chapter* – 2 with other experimental details. Urea with different concentrations (0.1 to 12 mol%) has been added separately. All the pure and doped ZTS solutions were continuously stirred for around 12 hours for homogeneous mixing of dopant. The saturated solutions were filtered in the separate beakers and these beakers with saturated solutions were mounted in a vibration free constant temperature bath with the constant growth parameters at 300 K for slow evaporation. The growth conditions were closely monitored. Within a span of 20 days, good quality pure and doped single crystals were harvested. The harvested pure and a typical urea (2.5 mol%) doped single crystals are shown in Fig. 7.2. From the photographs of crystals it is clear that crystals are visible quite transparent. The grown

crystals have been subjected to characterization for crystalline perfection and SHG investigations.

7.3 CHARACTERIZATION STUDIES

ZTS is a semiorganic material consisting of three molecules of thiourea and therefore the presence of doped urea was difficult to investigate by the conventional techniques such as, energy dispersive spectroscopy, CHN analysis, secondary ion mass spectroscopy (SIMS), atomic absorption spectroscopy, etc., because all the elements present in the dopant i.e. were already present in host material i.e. ZTS. The only distinguishing parameter for dopant from the host matrix was the presence of C=O functional group in urea which was different from C=S that of thiourea in ZTS. The FTIR is very sensitive to the presence/modification of functional groups in material and due to inability of above said techniques it has been used for characterization of crystals to evaluate the relative incorporation of urea into the host crystal lattice. The FTIR spectra for the crystalline specimens of pure and doped crystal were recorded at room temperature in the wavenumber range of 500-3500 cm^{-1} [§3.4]. The small single crystal specimens were used for the spectral recording.

Powder X-ray diffractometry is very sensitive to investigate the structural phases of the impurities in the crystals when the impurities are in large quantity and segregate to form the different phase from that of the host crystal. Therefore, to confirm the crystal structure and effect of doping and the crystallographic phase of the doped crystals the powder X-ray diffraction spectra of the pure, and 1.0, 5.0, 12.0 mol% urea doped crystals were recorded in the 2-theta range of 20 – 50 degree.

The influence of urea doping on the crystalline perfection of ZTS crystals has been revealed through the multicrystal X-ray diffractometer (Lal & Bhagavannarayana, 1989) by recording the diffraction/rocking curves (RCs) for all the pure as well doped specimens. The RCs for (200) planes of pure as well doped crystals were recorded performing ω-scan [§3.3]. In the present study, the X-ray power, size of the beam and configuration of the diffractometer were kept constant for all the specimens throughout the experiments. Before recording the diffraction curve,

to remove the non-crystallized solute atoms remained on the surface of the crystals and also to ensure the surface planarity, the specimens were first lapped and chemically etched in a non-preferential etchant of water and acetone mixture in 1:2 volumetric ratio. This minimal etching process also helps to get rid of the surface capping layers on the surface of crystals which generally get deposited due to the presence of complexating agents in the solution during the crystal growth process (Bhagavannarayana, Parthiban *et al.*, 2006).

Urea is an excellent SHG material and it is expected that the SHG behaviour of ZTS crystals must be improved with the doping of urea. The pure as well doped crystals were subjected to Kurtz powder method (Kurtz & Perry, 1968). The grown crystals were grounded to a uniform particle size of 125 – 150 μm, which is much more than that of the coherence length of laser beam [§3.13]. The urea and KDP crystalline powders were used as the standard to get the relative SHG efficiency of pure and doped specimens.

7.4 RESULTS AND DISCUSSION

7.4.1 Fourier transform infrared analysis

The concentration of the incorporated dopants in the crystal most likely not to be the same as in the solution due to the fact that while growing the crystal, it has a tendency to reject the foreign atoms or molecules to enter into the crystal lattice unless until they are chemically very favourable (like valancy, size, chemical/hydrogen bonding) and hence the real concentration of the dopants accommodated or entrapped in the crystal lattice may be much lesser but expected to be proportional to the prevailing concentration in the solution. Though, it is in principle possible to determine the true concentration in the crystal by sensitive characterization tools like atomic absorption spectroscopy, inductive coupled plasma, X-ray fluorescence spectroscopy *etc*. In the present case as the molecules of thiourea in the ZTS crystal and the molecules of urea (dopant) are similar and contain mostly the same atoms (C) or groups (NH_2) and hence these techniques could not yield the correct concentration of dopants.

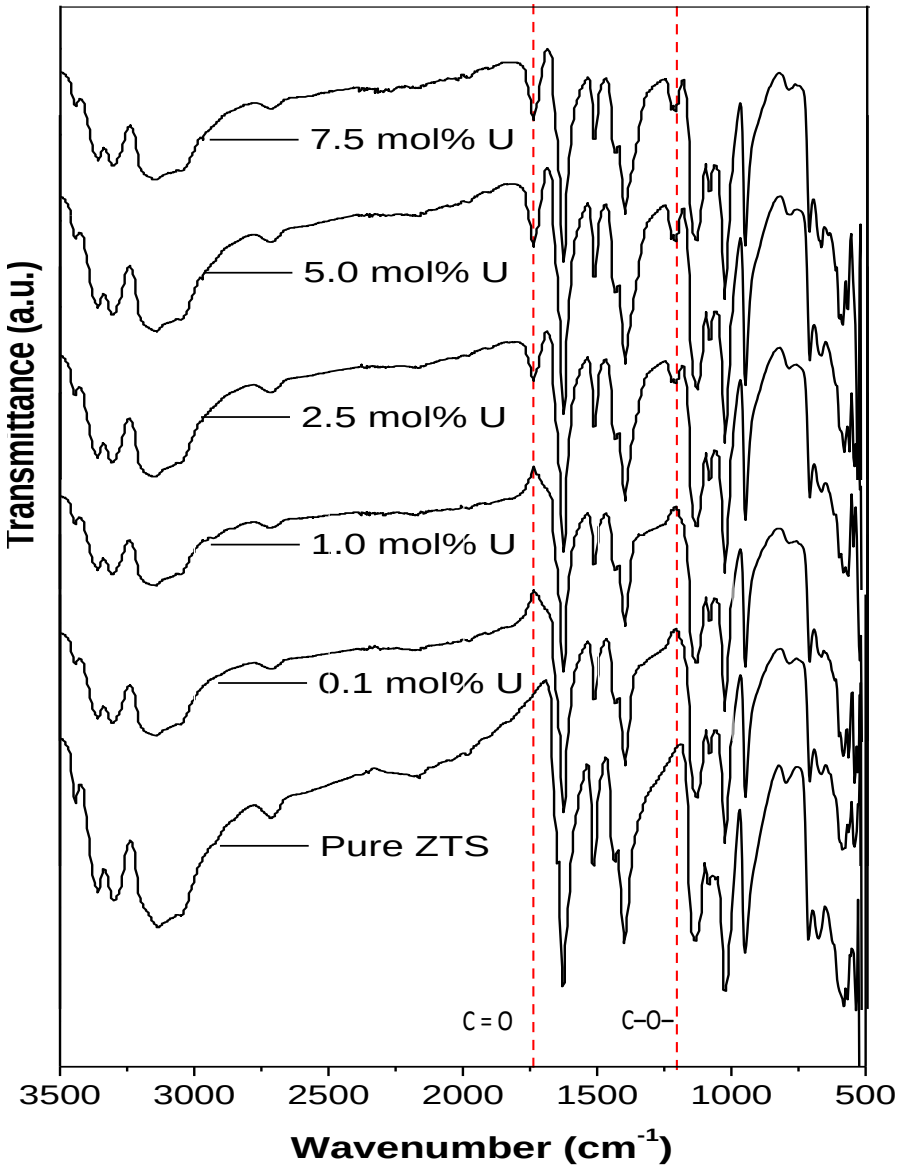

Fig. 7.3: *FTIR spectra for pure and different concentration urea (U) doped ZTS crystals. The red dotted lines indicate the positions of C = O and C – O stretching vibrations*

But using the stretched C=O bond in urea, one can not only confirm the presence of urea but also one can get an idea of relative quantity of incorporated urea in the crystal by the relative prominence of the absorption band in FTIR spectra. Figure 7.3 shows the FTIR spectra of pure and urea doped ZTS specimens growth with different concentrations ranging from 0.1 to 7.5 mol%, in the respective solutions. The peaks at 1628, 1502, 1404 and 714 cm^{-1} indicate NH_2 bending, N–C–N stretching, C=S asymmetric stretching and C=S symmetric stretching bonds respectively as expected in pure ZTS crystals (Meenakshisundaram *et al.*, 2006).

The observed absorption peaks at 1736 and 1210 cm^{-1} (as indicated by the dotted lines) indicate the stretched C=O and C–O bonds (Szetsen *et al.*, 1999; Wu *et al.*, 2003) respectively. The absence of shift of C=O absorption band indicates the incorporation of urea in the interstitial position instead of substitutional position. For pure and urea doped (0.1 and 1.0 mol%) crystals, the peaks are not well resolved. But above these concentrations, one can see the well resolved peaks with increasing prominence of these absorption bands due to increase in urea concentration. These features confirm the incorporation of urea in the crystalline matrix. The gradual increase in the prominence of these bands confirms the fact that due to increase in the concentration of urea in the solution, incorporation of urea in the crystal also proportionally increased. The occurrence of absorption band due to C–O indicates the presence of hydrogen bonds due to the presence of NH_2 groups of thiourea in ZTS matrix (Abhay Shukla *et al.*, 2001; Kohno *et al.*, 2003; Ning *et al.*, 1997). There are good number of examples in the literature (Xue & Zhang, 1970; Kato e*t al.*,1997; Xue & Zhang, 1996) which confirm that hydrogen bonding becomes the cause for the NLO nature of the crystals or helpful to enhance the NLO . The same result of enhancement of SHG has been observed experimentally in our present investigation as described in the forthcoming section and hence confirms the hydrogen bonding in urea doped ZTS crystals. These hydrogen bonds also help the entrapment of urea interstitially in the crystal and thereby help in enhancing SHG efficiency (Kato *et al.*, 1997) which is otherwise not possible as urea cannot occupy easily the substitutional position of thiourea. The investigations by powder XRD, HRXRD and SHG also confirm the same as described in the forthcoming sections.

7.4.2 Powder X-ray diffraction analysis

Before proceeding for the HRXRD studies, the PXRD analysis for undoped and urea doped specimens was carried out. The recorded PXRD for the pure as well doped crystals are shown in Fig. 7.4. The structure and the lattice parameters of both undoped and urea doped crystals were found to be the same as reported (Andreettie *et al.*, 1968). It is clear from the spectra that all the pure as well doped specimens contain a single phase of ZTS, as no extra peaks are observed. Except the minor variations in the peak intensities of different spectral lines due to strains,

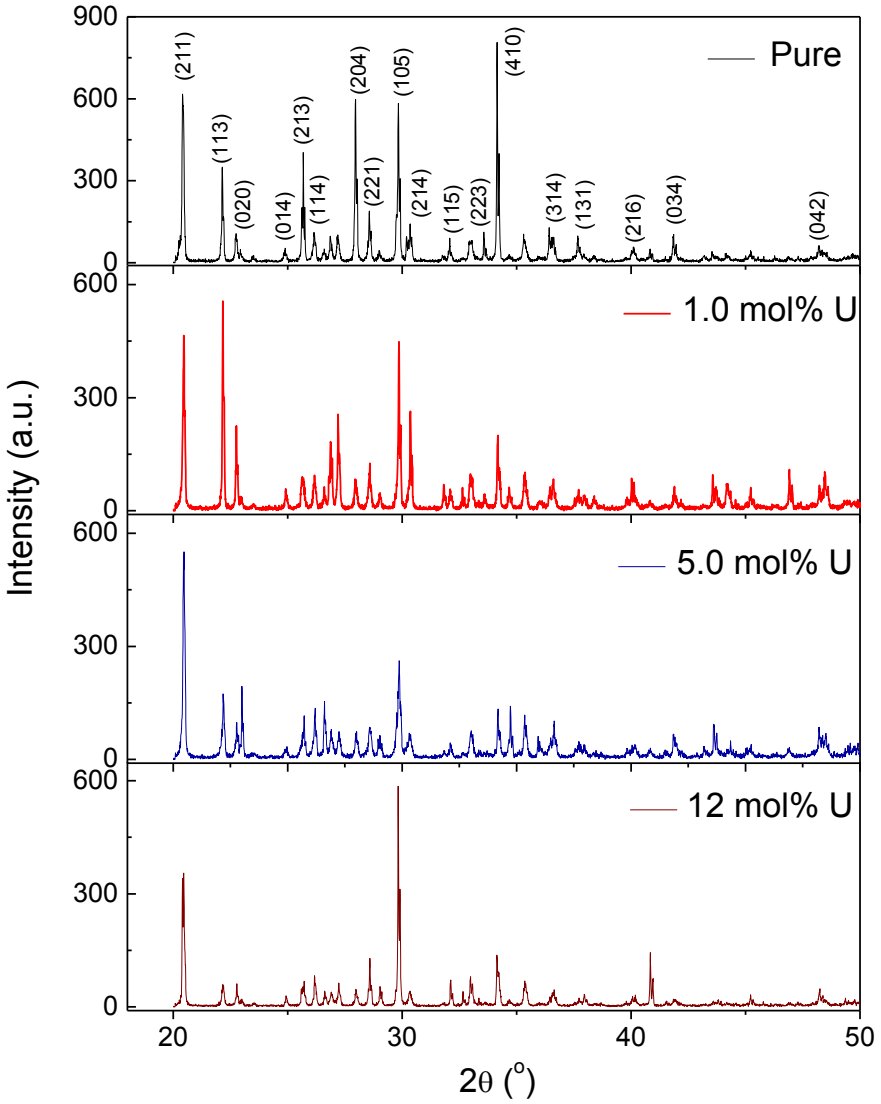

Fig. 7.4: *The PXRD spectra of pure as well urea (U) doped ZTS crystals*

neither additional phases nor significant variation in lattice parameters were found due to urea doping. The intensity of peaks for pure crystal is high and for the doped crystals the change in the intensity of the peaks taken place. This change in the peak intensities may be attributed to the changes in the lattice due to incorporation of dopants. The detailed investigation about the variations in the crystal lattice has been performed by HRXRD as described in the following.

7.4.3 High-resolution X-ray diffraction analysis

In order to analyze the effect of dopants on the crystalline perfection, high-resolution X-ray diffraction curves (RCs) were recorded [§3.3].

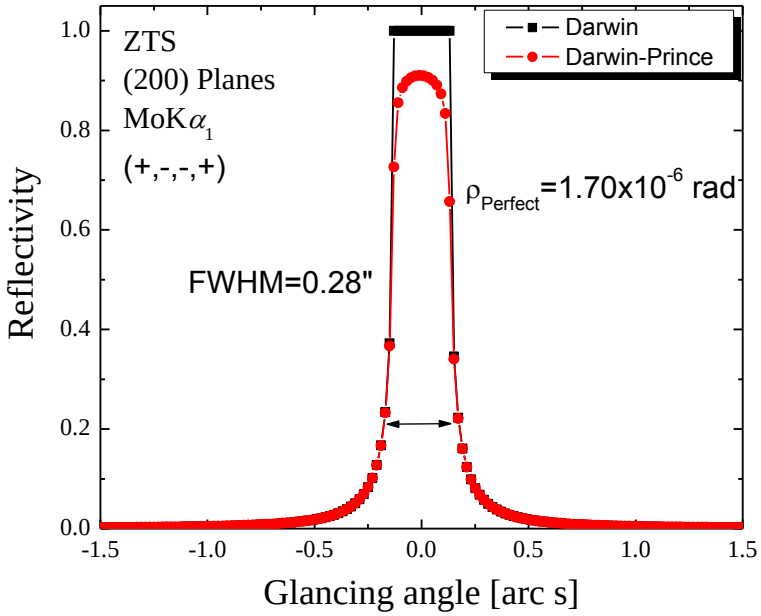

Fig. 7.5: *The theoretical Darwin and Darwin-Prince rocking curves for (200) diffraction planes generated using the plane wave theory of dynamical X-ray diffraction*

As shall be seen in the forthcoming analysis, depending upon the nature of RCs which in turn depend on the degree of concentration of dopants, the specimens are categorized in the following three groups: (i) Undoped specimen, (ii) Specimens doped with concentrations upto 2.5 mol% and (iii) Specimens doped with concentrations between 2.5 to 12 mol%. To assess the crystalline perfection of the grown crystals, one compare the shape and full width at half maximum (FWHM) of the experimentally recorded RCs with the theoretically obtained RCs. The *theoretical rocking* curves for (200) diffraction planes of pure ZTS crystal have been generated and are shown in Fig 7.5. These theoretical diffraction curves have been obtained with considerations of plane wave theory of dynamical X-ray diffraction (Batterman & Cole, 1964) for an ideally perfect crystal. The Fig 7.5 contains two diffraction curves; one called Darwin, where the phenomenon of linear absorption of X-rays is not considered and other called Darwin-Prince, in which the absorption correction is taken into account. From the diffraction curve (Fig. 7.5) it is observed that: (i) the reflectivity at the peak of the diffraction maximum is nearly 100% even in the Darwin-Prince curve and (ii) the intensity of the diffracted X-ray beam is appreciable only in a very narrow angular range, with half width of only 0.28 arcsec. High reflectivity and very low FWHM for the RC of ZTS is expected because most of the

elements in ZTS are light elements (Lesser the atomic number lesser the atomic scattering factor [§3.2]), which is otherwise higher for materials which contain elements with higher atomic numbers. For example the FWHM values are found to be ~ 9.5 arcsec for CdTe, 2.6 arcsec for $LiNbO_3$, ~ 0.6 arcsec for LiF. The integrated intensity (ρ) of the RC can be expressed in two ways depending on the nature of crystal. The ρ for an ideally *perfect* single block crystal is proportional to the structure factor as given by equation (6.3) [§6.4.3]. For a crystal having *mosaic* blocks it is proportional to the square of structure factor as given by the equation (6.2) [§6.4.3].

7.4.3.1 Undoped specimen

Figure 7.6 shows the RC for the undoped ZTS crystal recorded for (200) diffracting planes using Mo$K\alpha_1$ radiation in symmetrical Bragg geometry. The diffracted intensity of this curve and the other RCs described in current section as well as in §§7.4.3.2 and §§7.4.3.3 is an arbitrary, but the magnitude is relative. The experimental conditions like power and size of the X-ray beam are same and no normalization to either the peak area or the peak intensity is made. The range of the glancing angle for the RCs is so chosen to cover the meaningful scattered intensity on the both sides of the peak. The unit of glancing angle is in arcsec. It may be mentioned here that to assess the crystalline perfection one can choose any convenient set of planes which in turn covers the entire volume of the crystal.

ZTS specimens grow with major surfaces with (200) planes which have been used to record the RCs. The diffraction curve of Fig. 7.6 is quite sharp having FWHM of 5 arcsec with a good symmetry with respect to the exact Bragg diffraction peak position (set as zero). Such a sharp curve is expected for a nearly perfect single crystal as shown in Fig. 7.5. The sharp and single peak indicates that the specimen does not contain any internal structural grain boundaries (Bhagavannarayana *et al.*, 2005). The scattered intensity along the wings/tails on both sides of the exact Bragg peak (zero glancing angle) of RC is quite low, showing that the crystal does not contain any significant density of dislocations and point defects and their clusters (Lal & Bhagavannarayana, 1989). These features reveal that the quality of the pure ZTS is quite high.

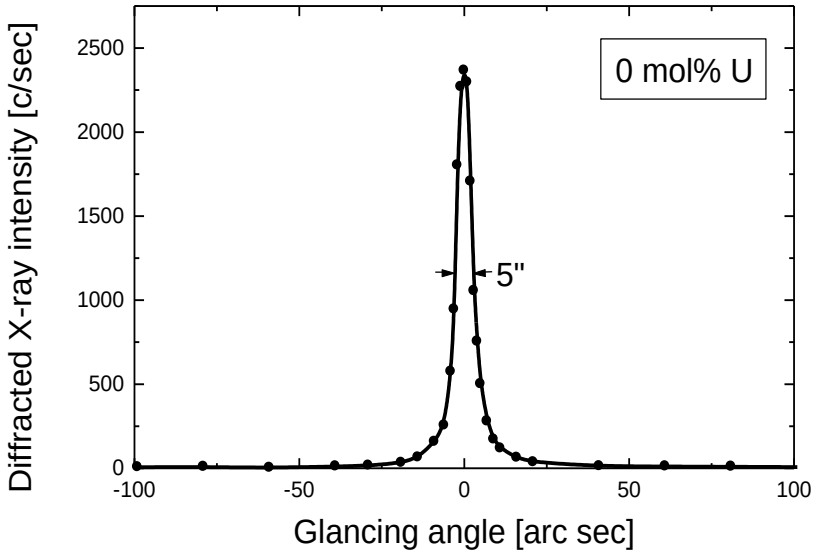

Fig. 7.6: *The high resolution X-ray diffraction curve recorded for (200) diffracting planes of the pure ZTS single crystal*

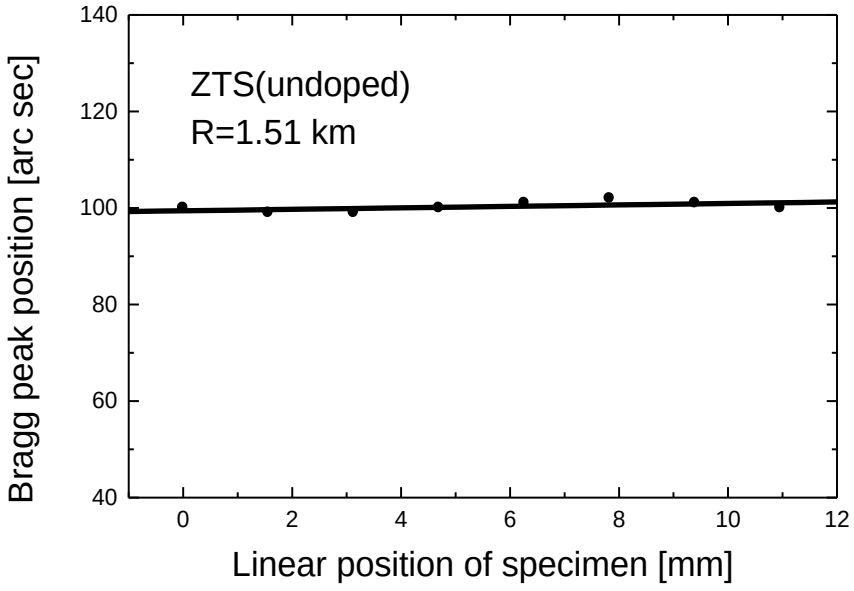

Fig. 7.7: *The radius of curvature plot for (200) diffraction planes of pure ZTS single crystal*

The quality is further tested by measuring the radius of curvature, described here.

To see the flatness of the crystallographic planes of the grown crystals, radius of curvature has been determined by recording the change in the diffraction peak position for the desired planes with respect to the linear position of the specimen as the specimen is traversed across the incident/exploring beam (Lal *et al.*, 1990). Figure 7.7 shows such a plot for same specimen as that of Fig. 7.6. It may be mentioned here

that the initial Bragg peak position which was set at 100 arc s is arbitrary and the slope does not depend on this value. The radius of curvature for (100) crystallographic planes of the specimen obtained by the reciprocal of slope of this plot is 1.51 km. This value is quite high which is expected for a good quality flat crystal (Sharma *et al.*, 2006). It may be mentioned here, the quantitative measurement of such flat crystals is not possible with the desired accuracy when the FWHM values are not low. In such a case the uncertainty in the location of peak position is high to determine quantitatively the value of radius of curvature for such flat crystals.

7.4.3.2 Specimens doped with concentrations up to 2.5 mol%

To analyze the effect of dopants in this range, three specimens with concentrations 0.1, 1.0 and 2.5 mol% were studied. The RCs of these specimens are shown in Fig. 7.8. As mentioned above, the relative diffracted X-ray intensity for all the samples is same as the experimental conditions like power and size of the X-ray beam are same and no normalization to either the peak area or the peak intensity is made. As seen in Fig. 7.8, all the three diffraction curves are having single peaks as in Fig. 7.6, confirming the fact that these doped specimens also do not have any structural grain boundary. However, the FWHM gradually increases as the urea (dopant) concentration increases. As seen in Fig. 7.8, FWHM values for the specimens with concentrations 0.1, 1.0 and 2.5 mol% respectively are 13, 18 and 21 arcsec. These are quite high in comparison to 5 arcsec belongs to the undoped specimen showing that the doping has a significant influence on the value of FWHM. On careful observation, one can also see that the intensity increases sharply as the glancing angle approaches the peak position as expected for a perfect crystal. But at higher glancing angles (away from the Bragg peak position), the scattered intensity falls down slowly. For the sake of convenient comparison, all these three RCs of doped specimens in Fig. 7.8 along with the RC of undoped specimen in Fig. 7.6 are combinedly drawn in Fig. 7.9 with a dotted vertical straight line at the exact Bragg peak position. A common range for the glancing angle from -100 to 100 is chosen for all the curves so as to see the asymmetry of the curves with respect to the peak position. From this figure one can clearly see that the intensity along the wings/tails of the RCs gradually increased as the dopant concentration increased.

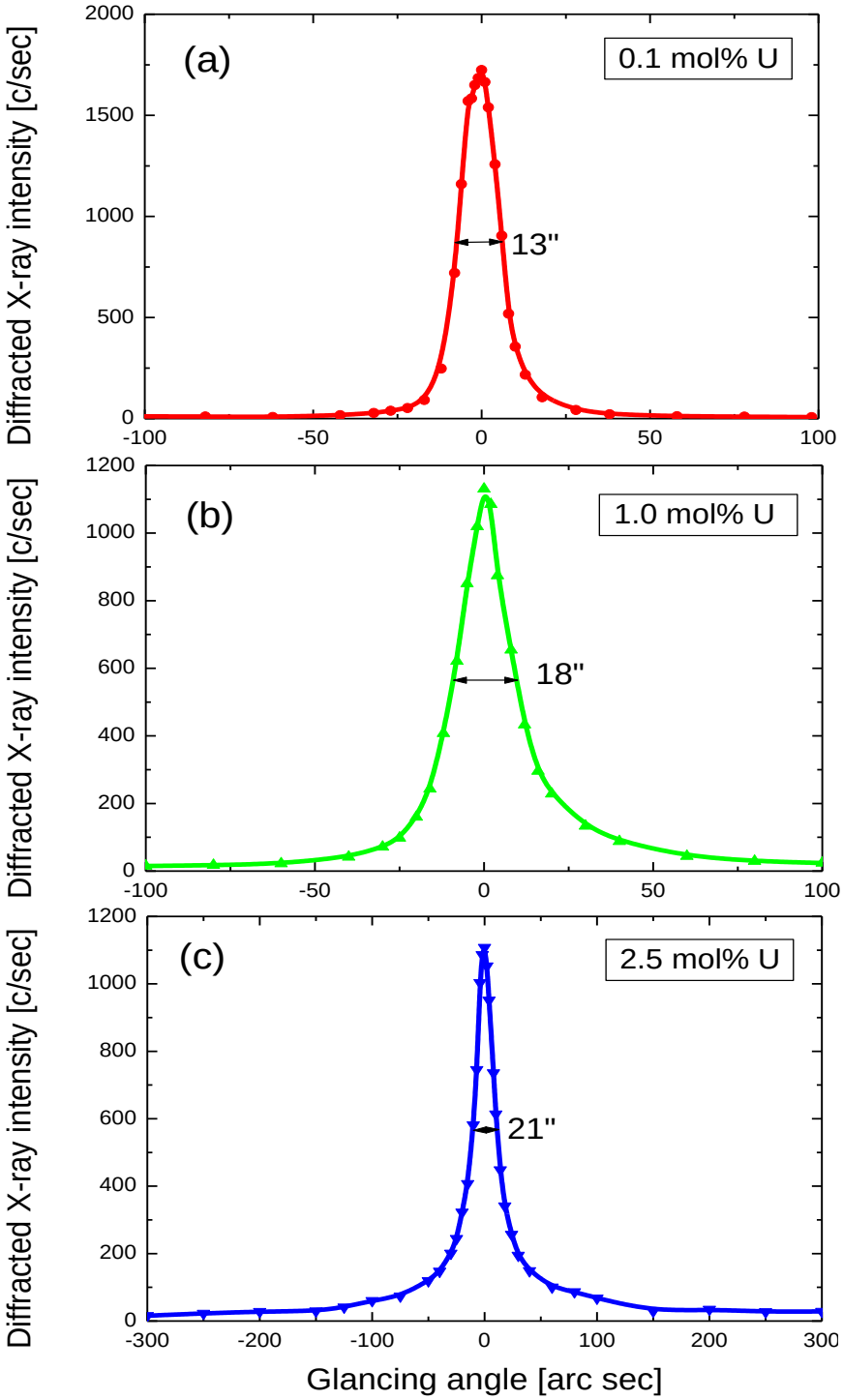

Fig. 7.8: *The high resolution X-ray Diffraction curves of doped ZTS single crystals recorded for (200) diffraction planes: (a) 0.1, (b) 1.0 and (c) 2.5 mol% urea*

The increase in FWHM without having any additional peaks indicates the incorporation of dopants in the crystalline matrix of ZTS. The gradual increase of FWHM and scattered intensity along the wings of the RCs as a function of prevailing concentration

of urea in the solution during the growth process indicate that the actual amount of urea entrapped (or doped) in the crystal is proportional to the concentration of urea present in the solution which is also in tune with the FTIR results.

It is interesting to observe few features of these curves: (i) the peak intensity, (ii) the area under the curve also known as integrated intensity 'ρ' and (iii) the asymmetry of the curves. The peak intensity of these curves rapidly decreases to 1 mol% and is saturated from 1 to 2.5 mol% whereas the FWHM value rapidly increases to 1mol% and is almost saturated from 1 to 2.5 mol% doping. However, ρ remains almost the same [§6.4.3]. The constancy of ρ with increase in dopant concentration indicates that the dopants are not agglomerated into clusters but statistically distributed in the crystal lattice. But the value of ρ for sample with 2.5 mol% is slightly higher than that of other specimens which indicates that this concentration is also slightly higher than that of the critical concentration up to which the dopants can stay in the crystal in isolated form without agglomeration.

In RCs of doped specimens, for a particular angular deviation ($\Delta\theta$) of glancing angle with respect to the peak position, the scattered intensity is relatively more in the positive direction in comparison to that of the negative direction. This feature or asymmetry in the scattered intensity clearly indicates that the dopants predominantly occupy the interstitial positions in the lattice and elucidates the ability of accommodation of dopants in the crystalline matrix of the ZTS crystal. This can be well understood by the fact that due to incorporation of dopants in the interstitial positions, the lattice around the dopants compresses and the lattice parameter d (interplanar spacing) decreases and leads to give more scattered (also known as diffuse X-ray scattering) intensity at slightly higher Bragg angles (θ_B) as d and sin θ_B are inversely proportional to each other in the Bragg equation ($2d \sin\theta_B = n\lambda$; n and λ being the order of reflection and wavelength, respectively which are fixed). It may be mentioned here that the variation in lattice parameter is only confined very close to the defect core which gives only the scattered intensity close to the Bragg peak. Long range order cannot be expected and hence change in the lattice parameters also cannot be expected as we could not found any change in powder XRD.

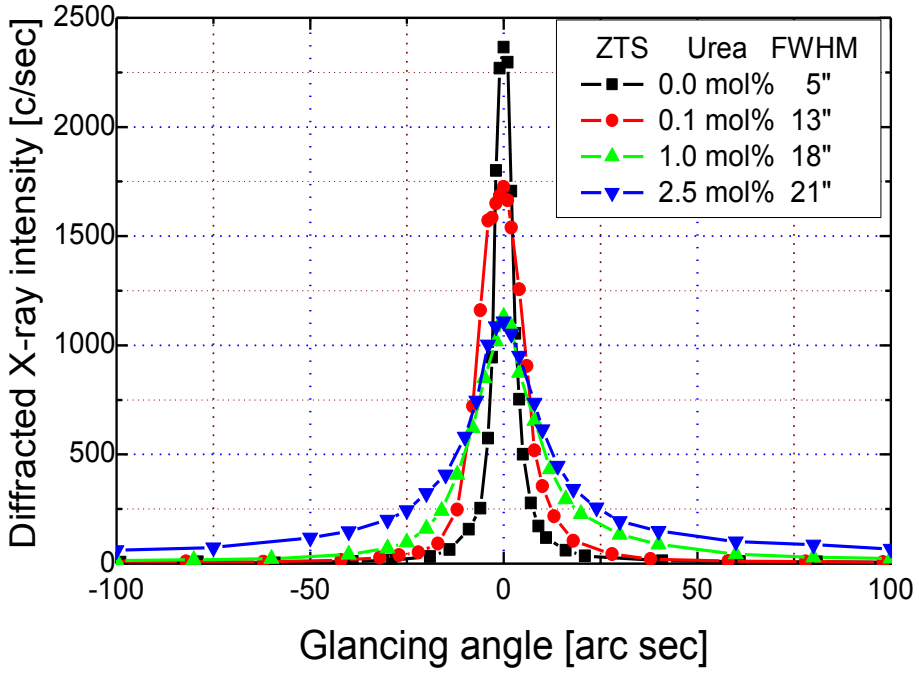

Fig. 7.9: *The comparative representation of diffraction curves for pure and doped (up to 2.5 mol%) specimens of ZTS crystals using (200) diffracting planes*

Entrapment of small amounts of dopants though they cannot substitute any host atom or molecule is possible due to their presence in the solution at large quantities. For molecules like urea in the host crystal like ZTS, the possible hydrogen bonds also help for their entrapment in small quantities. Entrapment in the interstitial positions is elucidated by the observed pronounced scattering on the higher diffraction angles with respect to the Bragg peak position. If urea would have taken the substitutional position of thiourea, lattice around the defect core (i.e. urea) might have widened (as S atoms in thiourea are larger than O atoms in urea) and experimentally one would get pronounced scattering on the lower diffraction angles. But experimentally, the other way is found and hence the occupation of urea in the interstitial position of the lattice with an associated compressive or compositional strain is a compatible conclusion of these findings. The correlation between dopant concentration with FWHM, ρ and asymmetry of the diffraction curve at lower amount of urea doping is indeed possible due to the high-resolution of the multicrystal X-ray diffractometer used in the present investigations. Otherwise one cannot distinguish such small variations in the FWHM particularly when the concentration of dopants or defects is very low.

As mentioned above, because of the entrapment of dopants (urea) in the interstitial positions of the crystal, the local region i.e. the region around the defect core undergoes compressive strain leading to reduction in the d spacing. Because of this, one expects scattering from the local Bragg diffraction from these defect core regions. Indeed, the *d* spacing of the whole crystal is not expected to change due to short range order of such strain. Therefore, omega scan used in the present investigation is good enough to collect all the scattered or local Bragg intensities due to such strained regions and can be attributed to the local compressive/compositional strain by the entrapped urea. Some more useful details may be found in our recent article pertaining to the studies on dopants in ADP crystals (Bhagavannarayana *et al.*, 2008). The effect of Cr^{3+}, Fe^{3+} and Al^{3+} on ADP crystals has been studied (Comer, 1959; Mullin *et al.*, 1970; Davey & Mullin, 1976) and it is known from Mossbauer studies (Fontcuberta *et al.*, 1978) that incorporation takes place at interstitial lattice sites.

7.4.3.3 Specimens doped with concentrations between 5 to 12 mol%

In this range of dopant concentration, the experimentally observed RCs contain additional peak(s). The curves (a), (b) and (c) in Fig. 7.10 show respectively the RCs of three typical specimens whose urea concentration is 5, 7.5 and 12 mol%. These RCs have quite different features than that of RCs in Fig. 7.6 and 7.8. In addition to the main peak at zero position, these curves contain additional peak(s). The solid line in the curves (a) and (b) which is well fitted with the experimental points is obtained by the Lorentzian fit. The additional peaks at 24 and 36 arcsec away from the main peak respectively in curves (a) and (b) are due to internal structural very low angle (≤ 1 arc min) grain boundaries (Bhagavannarayana *et al.*, 2005). The tilt angle *i.e.* the misorientation angle of the boundary with respect to the main crystalline region for these very low angle boundaries are 24 and 36 arcsec. Though these tilt angles (which are in arcsec) are very small, they indicate that the heavy compressive stress due to urea dopants at the high concentrations like 5 and 7.5 mol% lead to grain boundaries in the crystal. To rule out the possible other plane growth on the surface of crystals (Bhagavannarayana *et al.*, 2006), few micron surface layer of the crystal were ground and lapped before recording the RC.

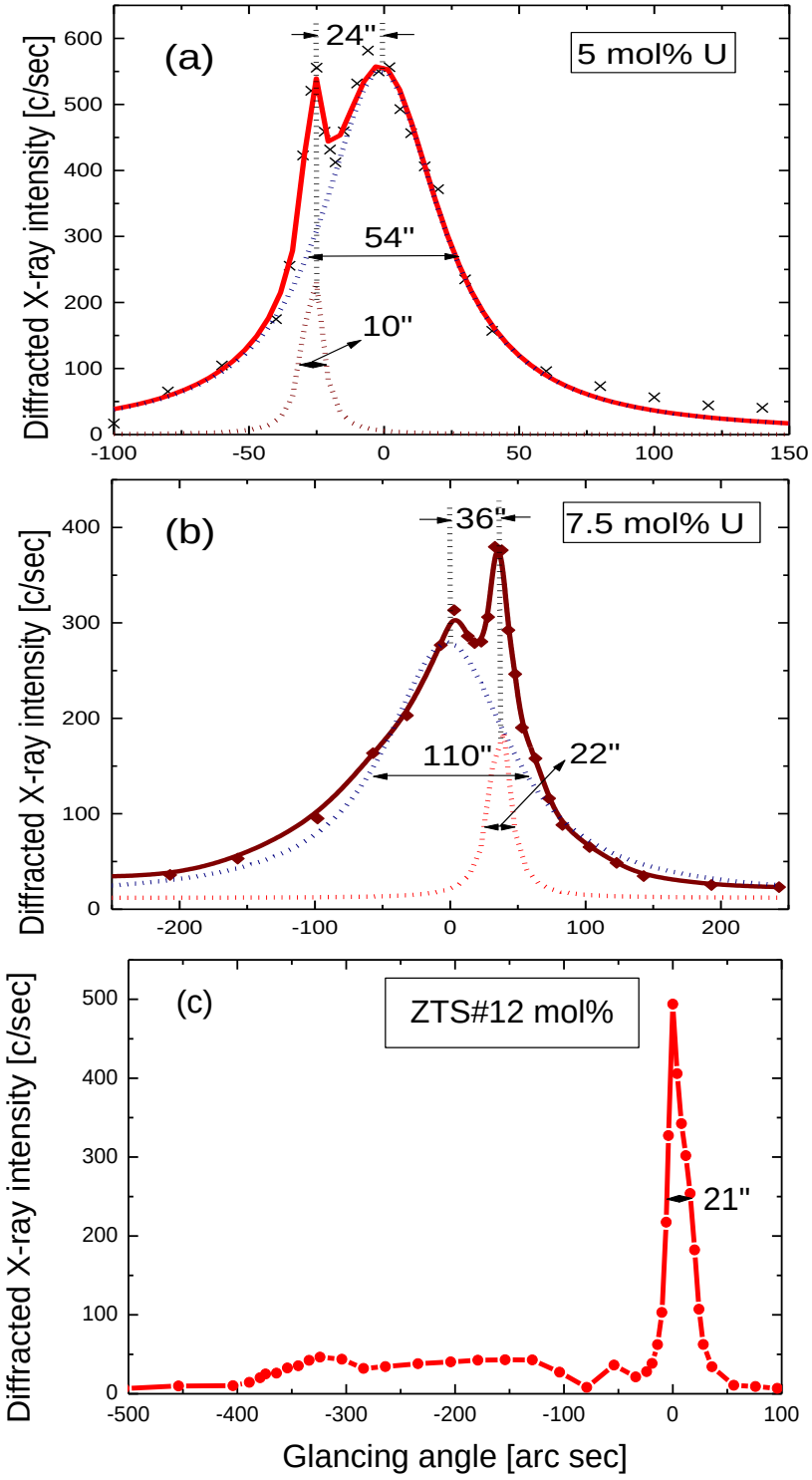

Fig. 7.10: *The high resolution diffraction curves Diffraction curves (a), (b) and (c) are for (200) diffraction planes of 5.0, 7.5 and 12 mol% urea (U) doped ZTS single crystals*

But still additional peak persists with the same tilt angle. Since the tilt angle is in the order of few arc seconds, one cannot attribute these grain boundaries as twins.

For further confirmation, section topographs were recorded separately at both the peaks of the RCs. As a typical example, for 5 mol% specimen, the section topographs were recorded separately at both the peaks of Fig. 7.10(a). The topographs indicted by I and II in Fig. 7.11 are respectively correspond to the very low grain boundary and the main crystal region. The grain type of dark background in this figure is due to poor resolution of photo occurred mainly because of the huge enlargement of the photograph. The size of the exploring X-ray beam on the X-ray film is 5 mm x 0.2 mm as indicated in the figure. As seen in the topographs, the intensity is not uniform along the length. In the left hand side, topograph belongs to the sharp peak at 24 arcsec, one can see good intensity on top portion. On the other hand, the bottom portion in the right hand side topograph contains more intensity. These observations indicate that the top and bottom crystalline regions of the specimen are mis-oriented by 24 arcsec and confirm the fact that the additional peak is due to a very low angle structural tilt grain boundary. Similarly, the additional peak in curve (b) also depicts the very low angle boundary. The high values of FWHM for the main peaks of these two specimens (having 5 and 7.5 mol% urea concentrations which are respectively 55 and 110 arcsec) indicate that the quality of these regions is not up to the mark. The large values of FWHM of the main peaks of curves (a) and (b) do not rule out the absence of mosaic blocks, which are misoriented to each other by few arc sec to few tens of arc sec. The consisting observation regarding FWHM is that more the dopant concentration, more its value. In these curves, it is also interesting to note down the lower FWHM values of 10 and 22 arcsec for additional peaks. Such low values of FWHM indicate that during the growth process, the entrapped dopants in the crystalline matrix slowly moved towards the nearby boundary and segregated along them. The heavy compressive stress seems to be the driving force for the movement of the excess dopants by the process of guttering. Such type of segregation of dopants along the boundaries was well confirmed in our earlier studies by SIMS on BGO crystals wherein the Si impurities were found to segregate along the structural grain boundaries (Choubey *et al.*, 2002). But the crystalline regions on both sides of the boundary contain some amount of dopant (urea),

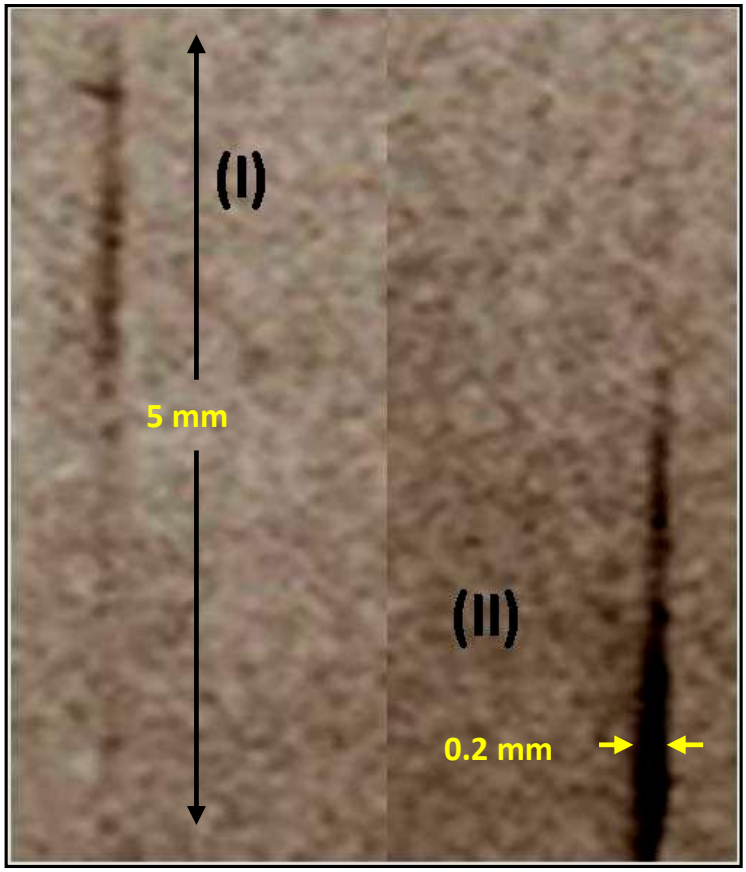

Fig. 7.11: *The section topographs recorded at the peak positions of the RC of Fig. 5.8 (a). The topographs at I and II respectively correspond to the very low angle grain boundary (at 24 arc s away from main peak) and the main peak (at zero position)*

which may be a critical concentration to accommodate in the crystal and is responsible for the observed enhancement of SHG compared to that of the undoped or doped crystals at low concentration as observed in the forthcoming section. The segregated urea however, cannot contribute anything for the enhancement as it does not exist in crystalline state though the urea itself is a good NLO material. But as mentioned above, the crystalline regions on both sides of the boundary which contains some entrapped urea in isolated form in the interstitial positions of the crystal contributes SHG of ZTS. However, such crystals with boundaries though they also show enhancement of SHG may not be of much use as the crystals needed for devices should be defect free for stability, reliability and full yield of SHG.

Curve (c) in Fig. 7.10 is the RC recorded for a specimen with 12 mol% urea. In the angular range between 100 to 500 arcsec, a mixture of unresolved low intensity

peaks can be seen and reveals the fact that the specimen contains a good number of mosaic blocks, which might be formed due to release of heavy stress aroused in the crystal from heavy doping. However, as in curves (a) and (b), this curve also contains one sharp peak which seems to be due to the denuded crystalline region from excess urea. As explained above such crystals are not good for device fabrication as crystals are anisotropic in nature and give full yield of their output only when all parts of the crystalline regions are having the same crystallographic orientation. The HRXRD results confirm an important finding that urea can be entrapped in the ZTS crystals, but the amount is limited to a critical value and above which the crystals have a tendency to develop structural grain boundaries. The excess urea entrapped in the heavily doped crystals seems to be segregated along the boundaries by the process of guttering and as a result of it; some regions are denuded from the excess dopants.

7.4.4 SHG efficiency analysis

As described in §7.3, SHG test on the powder samples was performed by Kurtz powder SHG method with the input radiation of 2.7 mJ/pulse. Output SHG intensities for pure and doped specimens give relative NLO efficiencies of the measured specimens. These values are given in Table 7.1 along with the output values of urea and KDP. As seen in the table, SHG output enhances considerably with the urea doping which is one of the most important findings of the present investigation. It is worth to mention here about the possible correlation of SHG output on crystalline perfection. As seen in the table, three distinct specimens of ZTS were chosen for the SHG measurements. As found in the HRXRD studies both undoped and 2.5 mol% urea doped ZTS are having good crystalline perfection.

Table 7.1: *The relative second harmonic generation (SHG) output*

Specimen	SHG output (mV)
Urea	715
KDP	119
ZTS undoped	143
ZTS doped with 2.5 mol% urea	242
ZTS doped with 7.5 mol% urea	287

Whereas, the 7.5 mole % urea doped specimen contains structural tilt grain boundaries which are detrimental to the NLO character as mentioned above. However, as seen in the table, urea doping enhances the SHG output irrespective of crystalline perfection. Our recent studies (Bhagavannarayana *et al.*, 2006) on ZTS and ADP crystals show a direct bearing of crystalline perfection on SHG efficiency. The controversy can be realized in the following way. In the present investigation, as observed in HRXRD studies, even in the heavily doped crystals, some portions (denuded regions from excess urea) of the crystal contains good crystalline perfection and contribute to the enhancement of SHG of the ZTS crystal. However, one should not ignore the crystalline perfection which deteriorates when the concentration is very high, due to formation of structural boundaries and leads to decrease in SHG efficiency as the total SHG yield from the different grains of the crystal with different orientation is expected to be less as SHG is anisotropic in single crystals.

7.5 CONCLUSION

The ZTS single crystals with different concentration of urea have been successfully grown by SEST. The crystal structure of the crystals has been confirmed by PXRD and it is found that doping did not change the crystals structure of ZTS and no extra peaks of the dopants have been observed in the recorded spectra. FTIR studies confirm the incorporation of urea dopant in ZTS crystal by adding urea in the solution while crystal is growing through slow evaporation of the solution. These studies also indicate the presence of hydrogen bonds in the doped crystals. From the HRXRD studies, it is clearly demonstrated that the crystalline perfection strongly depends on the dopant concentration. Depending upon the size and nature of the dopants, there is a limit of dopant concentration below which the crystal can accommodate. Above that limit, the dopants lead to develop structural grain boundaries and segregate along the boundaries by the heavy compressive stress in the lattice developed by them. Urea doping leads to increase SHG efficiency of the ZTS crystals substantially. It was also concluded that when we use certain dopants to increase the SHG efficiency of the host crystal, one should also cautious about the crystalline perfection as it deteriorates considerably (by the formation of structural

grain boundaries) at higher concentrations without much reduction in SHG efficiency particularly when the SHG output is measured by powder technique as observed in the present study. But in case of single crystals having structural boundaries, the total SHG output when measured in single crystal form certainly decrease as the SHG is a directional property of crystals.